

Accepted Article

Angle Fracture Repair

Fracture fixation technique and chewing side impact jaw mechanics in mandible fracture repair.

Hyab Mehari Abraha¹, José Iriarte-Diaz², Russell R Reid³, Callum F Ross⁴, Olga Panagiotopoulou^{1*}

¹Monash Biomedicine Discovery Institute, Department of Anatomy and Developmental Biology, Monash University, Victoria, Australia

² Department of Biology, The University of the South, Sewanee, Tennessee, USA

³ Department of Surgery, Section of Plastic Surgery, The University of Chicago Medical Centre, Chicago, USA

⁴Department of Organismal Biology and Anatomy, University of Chicago, Chicago, USA

*** Correspondence:**

Dr Olga Panagiotopoulou email: olga.panagiotopoulou@monash.edu

Running Title: Angle Fracture Repair

This article has been accepted for publication and undergone full peer review but has not been through the copyediting, typesetting, pagination and proofreading process which may lead to differences between this version and the [Version of Record](#). Please cite this article as doi: [10.1002/jbm4.10559](https://doi.org/10.1002/jbm4.10559)

This article is protected by copyright. All rights reserved.

Abstract

Lower jaw (mandible) fractures significantly impact patient health and wellbeing due to pain and difficulty eating, but the best technique for repairing the most common subtype—angle fractures—and rehabilitating mastication is unknown. Our study is the first to use realistic in silico simulation of chewing to quantify the effects of Champy and biplanar techniques of angle fracture fixation. We show that more rigid, biplanar fixation results in lower strain magnitudes in the implant plates, the bone around the screws, and in the fracture zone, and that the mandibular strain regime approximates the unfractured condition. Importantly, the strain regime in the fracture zone is significantly affected by chewing laterality, suggesting that both fixation type and the patients' post-fixation masticatory pattern—ipsi- or contralateral to the fracture—significantly impact the bone healing environment. Our study calls for further investigation of the impact of fixation technique on chewing behaviour. Research that combines in vivo and in silico approaches can link jaw mechanics to bone healing, and yield more definitive recommendations for fixation, hardware, and post-operative rehabilitation to improve outcomes.

Keywords: finite element analysis; mastication; rhesus monkey; mandible; maxillofacial surgery; trauma; implants

Accepted Article

Introduction

Mandible fractures have many causes, including congenital disorders, oropharyngeal cancers, falls (Ellis et al., 1985; Nasser et al., 2013; Kopp et al., 2016), battlefield injuries (Owens et al., 2008; Zachar et al., 2013), and vehicular accidents (Dimitroulis and Steidler, 1992; Schon et al., 2001). However, the single largest cause is interpersonal violence, mainly in young males who, in the USA and Australia, are disproportionately members of minority populations (Kruger et al., 2010; Afroz et al., 2015). Associated musculoskeletal disorders are a major cause of morbidity, with estimated hospitalisation costs in the USA of >\$5 billion (Pena et al., 2014), and further loss of quality of life and time off work during recovery (Butts et al., 2015). Treatment of mandible fractures aims to eliminate pain, promote bone healing, restore dental occlusion and jaw function, and improve facial aesthetics (Greenberg, 1993; Nasser et al., 2013; Kopp et al., 2016).

The most common mandible fracture site in adults is the angle region, extending from the corpus below the third molar (M_3) to the angle at the back of the mandible (Figure 1)(Schon et al., 2001). Clinical treatment of angle fractures usually involves open reduction and internal fixation (ORIF) using either one or two-miniplates (Greenberg, 1993). Single plate ORIF typically involves the Champy method: placement of one miniplate at the external oblique ridge, accessed trans-orally (Figure 1A) (Champy et al., 1975; Greenberg, 1993). Champy fixation is less rigid, allowing some motion at the fracture line, especially inferiorly, which is thought to promote indirect bone healing; i.e., callus formation followed by secondary bone formation and remodelling (Ghiasi et al., 2017). In contrast, more rigid ORIF of angle fractures involves two-miniplate, biplanar fixation in which the Champy method is augmented by the placement of a second miniplate on the inferior lateral surface of the mandible, accessed through a trans-buccal incision (through the cheek) with damage to the masseter muscle (Figure 1B) (Greenberg, 1993; Fox and Kellman, 2003). Biplanar fixation is more rigid, limiting micro-motion between bone fragments, but is thought to promote direct bone healing; i.e., direct connection and healing of bone fragments by osteoblastic and osteoclastic activity, but without callus formation (Nasser et al., 2013; Ghiasi et al., 2017).

There is an ongoing debate about whether Champy or biplanar fixation is the best treatment method of fixing angle fractures. The transoral approach used in Champy fixation is the least invasive and least disruptive to the masseter muscle, and is often argued to be associated with fewer complications (Ellis and Walker, 1994; Ellis and Walker, 1996; Al-Moraissi and Ellis, 2014) (but not always, e.g. (Schierle et al., 1997; Siddiqui et al., 2007)). Champy fixation is also assumed to result in more interfragmentary displacement (IFD, defined as the percentage change in interfragmentary distance, at the lower mandibular margin (Choi et al., 1995a; Shetty et al., 1995; van den Bergh et al., 2012), but it is unknown whether this movement is the right amount, yielding optimal healing times and fewer mal/non-unions, or too much, producing more mal/non-unions. Biplanar fixation certainly offers better mechanical stability than single plate fixation (Choi et al., 1995a; Chrcanovic, 2013), but it is unknown whether it *over*-stabilizes the fracture, reducing strain in the fracture line and inhibiting healing. It is also unclear which of these techniques best recovers the pre-fracture strain environment of the angle region, promoting fracture healing, and ensuring mandibular function.

Rhesus macaques serve as an excellent animal model to study the effect of different fixation techniques on the strain environment in the mandible. Our team has previously used a combination of *in vivo* experiments and computational modelling to study the biomechanics of the jaw in healthy rhesus macaques (Ross et al., 2011; Dechow et al., 2017; Panagiotopoulou et al., 2017; Orsbon et al., 2018; Mehari Abraha et al., 2019; Panagiotopoulou et al., 2020). We collected *in vivo* data on muscle activation, bone strain and three-dimensional (3D) jaw kinematics during chewing, combined these data with *ex vivo* measurements of bone material and muscle properties, and built a subject-specific, validated finite element model (FEM) of the macaque jaw during unilateral post-canine chewing

(Dechow et al., 2017; Panagiotopoulou et al., 2017; Mehari Abraha et al., 2019; Panagiotopoulou et al., 2020). We tested a series of hypotheses about loading regimes (*the combination of external forces acting on the mandible*), deformation regimes (*the change in mandible shape*), and stress and strain regimes (*patterns of internal forces and strains associated with loading and deformation regimes*) in the unfractured mandible, including the corpus-ramus junction—the region where angle fractures occur (Mehari Abraha et al., 2019). As in humans (Korioth et al., 1992; Korioth and Hannam, 1994), during simulated unilateral chewing in healthy macaques the balancing (non-chewing) side mandibular corpus is twisted about its long axis such that the alveolar process is inverted, negatively bent (concave inferiorly), and negatively sheared in sagittal planes (Panagiotopoulou et al., 2020). On the working (chewing) side the posterior corpus is twisted about its long axis such that the alveolar process is everted, positively bent and negatively sheared in sagittal planes, and laterally bent in transverse planes (Panagiotopoulou et al., 2020). The macaque mandible's overall deformation pattern is remarkably similar to that of humans (Korioth et al., 1992; Korioth and Hannam, 1994; Panagiotopoulou et al., 2020), supporting the use of the macaque mandible as a model of human jaw function.

In this study we used this model of our healthy control to compare the impact of the Champy and biplanar angle fracture fixation techniques on the strain regime in the titanium plates, in the bone around the implant screws, in the bone around the fracture, and in the mandible globally. *In silico* we simulated a fracture in the left angle then repaired it with models of titanium 64-alloy miniplates (26.1 mm x 2.5 mm x 1 mm) and bone screws using either the Champy or biplanar fixation techniques. The models were assigned the same tissue material properties, boundary conditions, and muscle forces as the healthy control then loaded to simulate chewing ipsilateral and contralateral relative to the fracture. (Figure 2). We compared the effects of fixation technique on the moments acting on the mandible, as well as on strains in the titanium plates, the bone around the screws, the bone on either side of the fracture, the fracture gap itself, and the mandible more distant from the fracture.

With respect to Champy fixation, we hypothesised that:

- because Champy fixation concentrates the load path through a single plate it would significantly alter the loading regime of the fractured mandible and be associated with higher principal strains at the bone-implant interfaces;
- because it is the least rigid, it would be associated with the largest inter-fragmentary movement at the fracture gap (Choi et al., 1995b; Shetty et al., 1995; Fedok et al., 1998; Chrcanovic, 2013);
- and because the presence of the fracture redirects the load path through the implant construct, Champy fixation would reduce strains (strain shielding) around the fracture zone, particularly inferiorly.

With respect to biplanar fixation, we hypothesized that:

- because biplanar fixation transfers load through two plates, it would have less effect on the loading regime of the fractured mandible and would be associated with lower strains at the bone implant interfaces.
- because it is the most rigid fixation, it would be associated with the least inter-fragmentary movement.
- and because the presence of the fracture redirects the load path through the implant construct, biplanar fixation would result in strain reduction around the fracture zone both inferiorly and superiorly.

Methods

Macaque Finite Element Models (FEMs)

Healthy Control

We modified our previously published and validated subject specific FEMs of healthy macaque chewing to simulate the two fracture fixation treatments (Champy vs biplanar) (Panagiotopoulou et al., 2017; Mehari Abraha et al., 2019).

In brief the 3D geometry of the macaque mandible and cranium was captured using computed tomography (CT) on a Philips Brilliance Big Bore scanner at the University of Chicago (Panagiotopoulou et al., 2017) (Figure 2A). The scans were processed in Mimics v17 software (Materialise, Leuven, Belgium) using manual and automatic segmentation methods to separate the cranium from the jaw and create 3D surface data of the mandibular tissues of interest (trabecular tissue, cortical bone, teeth and anterior bone screws) (Panagiotopoulou et al., 2017) (Figure 2B). The periodontal ligament was excluded from our analyses because it does not impact global strain regimes and increases computational time (Mehari Abraha et al., 2019). The 3D surface files of the different tissues of the healthy control were imported into 3-matic v15 (Materialise, Leuven, Belgium) to create a 3D non-manifold assembly, converted into volumetric mesh files of linear tetrahedral elements, then imported into Abaqus CAE Simulia (Dassault Systèmes, Vélizy-Villacoublay, France) software for modelling. All mesh details are provided in Supplementary Table 1.

Isotropic, homogeneous, and linear elastic material properties were assigned to the teeth ($E=24.5$ GPa; $v=0.3$) and trabecular bone tissue ($E=10$ GPa; $v =0.3$). The cortical bone was modelled as heterogeneous and orthotropic using our published measurements of bone properties (Dechow et al., 2017) adjusted to the radiodensity of the calibrated CTs (Dechow et al., 2017; Panagiotopoulou et al., 2017). Tie constraints were used to bind together intersecting surfaces in the models to eliminate friction, known to influence FEA results (MacLeod et al., 2012).

Experience suggests that realistic strain regimes (including lateral transverse bending) are obtained by fixing the working (chewing) side mandibular condyle against displacement in all directions and the balancing (non-chewing) side condyle in anterior-posterior and superior-inferior directions only; the balancing condyle was allowed mediolateral translation to simulate lateral wish-boning of the mandible during the power stroke of mastication. Bite forces resulted from constraining nodes on the occlusal surfaces of the chewing side premolars and first molar against all translations (Panagiotopoulou et al., 2017; Mehari Abraha et al., 2019; Panagiotopoulou et al., 2020). Models were loaded using muscle activity data collected *in vivo* (Supplementary Data 1) (Panagiotopoulou et al., 2017). To apply muscle forces, for each jaw muscle (anterior & posterior temporalis; deep & superficial masseters; medial pterygoids) surface nodes representing the origin and insertion were selected on mandible and cranium, a directional vector joining the origin and insertion centroids was calculated, and these vector components were used to assign muscle force orientations at the mandibular insertion nodes (Panagiotopoulou et al., 2017; Panagiotopoulou et al., 2020). Magnitudes of the muscle forces were estimated as the mean normalised EMG amplitude \times estimated muscle physiological cross-sectional area (PCSA) \times specific tension of muscle (30 N/cm 2) (Sinclair and Alexander, 1987; Panagiotopoulou et al., 2017; Mehari Abraha et al., 2019; Panagiotopoulou et al., 2020). PCAs published in (Panagiotopoulou et al., 2017) were used. FEM solution of all models was performed using the Abaqus direct implicit static solver.

Treatment FEMs

To simulate angle fracture on the healthy control for the current study, we used 3-Matic v15.0 and created a 0.2 mm planar cut in the angle of the left side mandible. The fracture line was then repaired with two different techniques Champy and biplanar (Figure 2C) fixation using 26.1 mm x 2.5 mm x 1

mm locking (threaded) miniplates with 4.2 mm self locking screws. We have not geometrically modelled a thread in the miniplate. Instead, we bound the internal surface of the screw head to the plate to mimic a thread. The components of each model (cortical bone, trabecular tissue, teeth, miniplates and screws) were then collated into a non-manifold assembly (Figure 2C), converted to volumetric .inp files and exported to Abaqus Simulia CAE 2016 for solution. All mesh files passed standard 3-Matic and Abaqus 2016 element quality checks. All mesh details are provided in Supplementary Table 1. A close view of the 3D mesh of the bone interface and fracture zone of Champy and Biplanar FEMs is provided in Supplementary Figure 1. The mandible was assigned the same material properties as the healthy control (Figure 2D). All implant materials (anterior bone screws, miniplates, fixation screws) were modelled as isotropic and homogeneous ($E=105\,000\text{ MPa}$; $\nu=0.36$) (Kraaij et al., 2014; Panagiotopoulou et al., 2017).

The interfaces between adjacent biological surfaces (cortical bone-teeth, trabecular tissue-teeth, trabecular tissue-cortical bone) were modelled as tie constraints (surface to surface interaction with no relative motion). All screw-bone surfaces were modelled as tie constraints (to replicate screw threads bonded to bone). The surface interactions between cortical bone, miniplates and screws and between fracture segments were defined as 'hard' contacts, with a penalty static friction coefficient of 0.3 (Shockey et al., 1985; MacLeod et al., 2012; Fuh et al., 2013; Damm et al., 2015; Voutat et al., 2019).

Like the healthy control all FEMs were solved using in Abaqus CAE default implicit direct static solver (Dassault Systèmes, Vélizy-Villacoublay, France) (Figure 2E). Average solution time (6 processors and 8 tokens) was ~30 min per model.

Numerical Comparison

When calculating the maximum strain values in the bone implant interface and in the implant tissues, we excluded nodes that reported strains outside two standard deviations from the mean (excluded top and bottom 5% of values). This was to ensure that elements with very low aspect ratios were excluded from any numerical comparison, as they report unrealistic strain results ($\sim 45,000\mu\epsilon$) that are likely an artefact of the interface between cortical bone and the plate construct.

The resultant moments in Abaqus were calculated about coordinate axes through centroids of cross sections. As a result, the moments in each of the sections are moments about a point in the local coordinate system, given by the sum of all moments due to the internal forces acting at the section relative to the local coordinate system origin.

Results

In macaques (as in humans) (Panagiotopoulou et al., 2020) the largest moments acting on the angle region are sagittal bending moments, and these are higher during contralateral chewing than in ipsilateral chewing (Figure 3). Fracture fixation technique had little impact on the loading regime of the mandible during ipsilateral chews, but it greatly altered moments acting around the fracture plane during contralateral chews (Figure 3; Supplementary Video 1). Champy fixation had the greatest effect, effectively eliminating anterior-posterior (AP) twisting moments (moments about Y) acting on the mandible immediately in front of and behind the fracture, eliminating sagittal bending moments just in front of the fracture, and halving sagittal bending moments just behind the fracture (Figure 3). Moreover, the Champy technique also altered the loading regime along the entire length of the corpus between the fracture and the symphyseal region during contralateral chews (Figure 3), changing the AP twisting moments from positive to negative and significantly increasing their magnitude (Figure 3).

These changes to the loading regime are reflected in changes in the strain environment both in and around the implants and fracture, and were strongly impacted by whether chewing occurred ipsilateral or contralateral to the fracture. As predicted, concentration of the load path through a single plate under Champy fixation resulted in higher principal strain magnitudes in the plates and in the bone-screw interface than under biplanar fixation, especially under chewing contralateral to the fracture (Figure 4A & Table 1). This concentration of the load path through the plates and screws was accompanied by significant strain shielding (lower ϵ_1 and ϵ_3 strain magnitudes compared to the healthy, blue colors in Figure 4B) around the lower third of fracture during contralateral chewing after either Champy or biplanar fixation (Figure 4B). We also found very low von Mises stresses (<80 MPa) in the bone implant interfaces with high stresses (>150 MPa) only localised in the titanium plate. Miniplate von Mises stresses were the highest in the Champy fixation condition and during contralateral chews (Supplementary Figure 2). Elsewhere around the fracture, both fixation techniques resulted in decreases in one principal strain magnitude (ϵ_1) and increases in the other (ϵ_3).

Within the fracture plane itself there were marked differences in interfragmentary displacement between Champy and biplanar fixation, and significant departures from traditional expectations (Figure 5). Not surprisingly, the less rigid Champy fixation was associated with the greatest overall change in interfragmentary distance (Table 2), with an approximately 80% reduction in interfragmentary distance (IFD), indicative of almost uniform compression of the fracture during ipsilateral chewing. Contralateral chewing after Champy fixation was accompanied by an unexpected lateral bending of the fracture—tension medially (>80% fracture gap widening) and compression laterally (>80% gap distance shortening) (Figure 5). As expected, the more rigid biplanar fixation resulted in a fracture zone that was essentially static (<10% change in IFD) during ipsilateral chewing, but the same lateral bending was seen during contralateral chewing, albeit to a lesser degree than following Champy fixation (Figure 5).

Fixation technique also impacted strain regimes in the rest of the mandible, away from the fracture zone (Figure 6). These effects were small during chewing ipsilateral to the fracture, with strains after both biplanar and Champy fixation deviating by <100 $\mu\epsilon$ from the healthy control. However, during chewing contralateral to the fracture, fixation technique significantly impacted strains away from the fracture zone and these effects were large (Figure 6). In the Champy model, the greatest deviations, >400 $\mu\epsilon$ from healthy strains, were found in the labial and lingual faces of the right side parasymphysis (ipsilateral to the bite point and contralateral to the fracture), and in the lingual aspect of the left corpus (Figure 6). In contrast, the biplanar fixation model only deviated substantially from the healthy control in the labial right parasymphysis, immediately below the loaded teeth (P3-M1), and in a small area of the lingual left parasymphysis (Figure 6).

Discussion

Our results show that the more rigid biplanar fixation technique is associated with the smallest changes in the loading regime acting around the fracture, the lowest strains in the titanium plates, the lowest strains in the bone-implant interface, the least interfragmentary displacement, and a global mandibular strain regime that best matches the healthy control. This is especially true during contralateral chews, when the second lateral plate is well placed to resist the high sagittal bending moments acting across the fracture plane. Single plate Champy fixation results in higher strains in the plate, higher strains at the bone implant interface, high degrees of interfragmentary displacement, and global strains that deviate substantially from the healthy control, particularly during contralateral chews (Supplementary

Video 1). Increased strains in the plate may be an artefact of the locking screws used. Clinically, in the majority of Champy plate fixations the plates and screw are non locking. Due to lack of data on the coefficient of friction required to model the non locking screws, we optimised the plates and screws virtually so that they conform to the body surface and modelled the plate-screws for the Champy fixation as locking. Future *in vivo* research will allow us to measure the friction coefficient at the bone implant interface experimentally and further optimise the modelling of the hardware for our treatments. Notably, Champy fixation leads to dramatic variations from healthy strains in areas far away from the fracture zone (e.g. right lingual parasympysis). This finding suggests that the lack of rigidity present following Champy fixation not only fails to stabilize the fracture plane, but also results in changes to the global strain environment of the jaw.

Understanding the mechanical environment of the jaw post fracture and fixation is an essential prerequisite for designing repair and rehabilitative techniques that optimize patient outcomes (Rudderman et al., 2008). In order to understand how the mechanical environment of the jaw impacts healing, we first need to understand how different fixation techniques affect jaw mechanics (Tams et al., 1996; Rudderman et al., 2008). This study used finite element analysis to test the impact of the two most clinically widespread angle fracture fixation techniques (Champy and biplanar) on strains in and around implants and the fracture zone during chewing. We found that because fracture fixation redirects the load path almost exclusively through the plate construct the less rigid, single plate Champy fixation technique is associated with higher principal strains in the plate and the bone-screw interface than the biplanar technique. This effect is exacerbated by chewing on the opposite side to the fracture, when sagittal bending moments acting on the fracture plane are greatest. Our results are consistent with those of Liu et al. (2017), who found that single plate fixation is associated with higher stresses in the bone implant interface and the implant construct than two plate fixation.

If Champy fixation results in such a biomechanically unfavourable environment, why is it so successful clinically (Ellis et al., 1985)? The widely accepted explanation is that Champy fixation is less invasive than biplanar, especially in causing less disruption of masseter (Ellis et al., 1985; Schierle et al., 1997), but how the two techniques affect muscle activity during feeding after fracture fixation is unknown. In this study we used muscle loadings based on muscle recruitment patterns measured in healthy controls because the only available data on the impact of fixation technique on feeding system function are bite force data and EMG activity from easily accessible muscles during transducer biting (Tate et al., 1994; Gerlach and Schwarz, 2002; Bither et al., 2012). Data are urgently needed on post-fracture jaw muscle activity and jaw kinematics during chewing to evaluate the potential for rehabilitative treatments for speeding healing and functional recovery.

One of the most salient results of this study is the importance of the laterality of post-fracture mastication. Our results show that contralateral chewing following Champy fixation is associated with much greater degrees of interfragmentary displacement (50% and 162%) than the optimal window of 10% suggested by orthopaedic literature (Hente et al., 2001; Perren, 2002). This suggests that mobile less rigid fixation and contralateral chewing behaviour may inhibit bone healing and contribute to the development of post-operative complications, such as non-union or malunion of the fracture segments (Passeri et al., 1993). In contrast, ipsilateral chewing following either fixation technique generates strain regimes in the fracture zone that most closely resemble the healthy control. Hence, ipsilateral chewing using healthy control muscle recruitment patterns might speed healing success in *isolated* angle fractures. However, it is important to note that Champy fixation is accompanied by dramatically increased principal strains in the parasympyseal region contralateral to the angle fracture, particularly during contralateral chews. This is exactly the location of the most common fracture occurring in combination with an angle fracture (Dongas and Hall, 2002; Czerwinski et al., 2008). Hence, rehabilitation strategies for isolated angle fractures may actually be contra-indicated for multiple

fractures involving angle and parasympheal regions. Clearly better data are needed on the impact of fracture fixation technique on muscle activity and mandibular loading and strain regimes.

Previous comparisons of angle fracture fixation techniques using benchtop experiments on cadaveric or resin based human mandibles have not replicated physiological loading conditions and have yielded conflicting results (Choi et al., 1995a; Haug et al., 1996; Alkan et al., 2007). By using a computer simulation environment and loading our finite element models with physiologically accurate muscle forces, our study is the first to simulate the strain environment in and around the fracture and implants during use of the jaw for its primary function—chewing. Thus our finite element models are the most robust testing environment for different angle fracture fixation techniques developed to date. Our results suggest that biplanar fixation should yield the best healing outcomes, but we hesitate to make firm recommendations until we can load our fracture-fixed finite element models with muscle forces estimated using data from subjects with surgically repaired mandible fractures. Patients with repaired mandible fractures may change muscle force activation patterns consciously in response to pain or unconsciously in expectation of pain (Gerlach and Schwarz, 2002; Butts et al., 2015). To our knowledge no study has characterized the subject-specific pre- and post-fixation muscle activation patterns of all the major muscles of mastication during chewing. Incorporation of post-fixation behavioural plasticity into models of the post-fixation biomechanical environment of the jaw would significantly expand the translational reach of our modeling. Addressing these limitations and clarifying the relationship between fracture, treatment (fixation), behavioural plasticity and healing are essential to the design of optimized treatment methods for angle fractures. Research integrating *in vivo* data with accurate *in silico* models offers the best opportunity to circumvent issues common with existing clinical research, such as variation in patient compliance, surgical expertise, and postoperative therapy. Only by combining *in vivo* experiments, biomechanical modelling and histological measures will we obtain a clearer understanding of the relationship between specific techniques of angle fracture fixation and bone healing in the mandible.

Data Availability Statement

Submission (.inp) and results files (.odb) for all finite element models presented in the main text⁵⁹ and in the supplementary material⁶⁰ can be found on Monash Bridges at <https://figshare.com/s/a46efafc1f4581db1001> and <https://figshare.com/s/e942ed9d539f9e1ea74c> respectively. All muscle data used as part of this publication can be found in the Supplementary Data 1. All data analysis files, including raw data from Abaqus (.rpt) and analysis code, for the main text and supplementary material can be found on Monash Bridges at <https://figshare.com/s/f7d8816fba6b72dc5f45> and <https://figshare.com/s/20535cedf405e83707e6> respectively. Data analysis files are organised by Figure and table number.

Code Availability Statement

Custom MatLab and R code was written by Hyab Mehari Abraha to conduct inter-fragmentary distance and coefficient of static friction sensitivity analysis for all models. Code is available on Monash bridges for analysis conducted on the main text and supplementary material on Monash Bridges at <https://figshare.com/s/f7d8816fba6b72dc5f45> and <https://figshare.com/s/20535cedf405e83707e6> respectively. Custom MatLab code was written by Jose Iriarte-Diaz to conduct the whole model nodal comparisons of all models. Code is available at <https://github.com/josdiiri/plotSurfaceStrains/>.

Acknowledgements

The work was supported by internal funds from Monash University and Monash Biomedicine Discovery Institute to OP. We thank Dr Wencheng Lui (University of Shanghai for Science and Technology) and Associate Professor Bernard Chen (University of Melbourne, Department of Mechanical Engineering) for useful discussions. We thank the anonymous reviewers and the editors for constructive feedback.

Author Contributions

OP, CFR , RR and HMA designed the experiments. OP and HMA built the FE models. HMA and JID, analysed data; HMA, OP, CFR and RR wrote the paper.

Conflicts of Interest

We declare we have no competing interests.

References

- Afrooz PN, Bykowski MR, James IB, Daniali LN, Clavijo-Alvarez JA. 2015. The Epidemiology of Mandibular Fractures in the United States, Part 1: A Review of 13,142 Cases from the US National Trauma Data Bank. *J Oral Maxillofac Surg* 73:2361-2366.
- Al-Moraissi EA, Ellis E, 3rd. 2014. What method for management of unilateral mandibular angle fractures has the lowest rate of postoperative complications? A systematic review and meta-analysis. *J Oral Maxillofac Surg* 72:2197-2211.
- Alkan A, Metin M, Muglali M, Ozden B, Celebi N. 2007. Biomechanical comparison of plating techniques for fractures of the mandibular condyle. *The British journal of oral & maxillofacial surgery* 45:145-149.
- Bither S, Mahindra U, Halli R, Bakshi M, Kini Y, Shende M, Bither R. 2012. Electromyographic analysis of anterior temporalis and superficial masseter muscles in mandibular angle fractures--a pilot study. *Oral Maxillofac Surg* 16:299-304.
- D'Ants SC, Floyd E, Lai E, Rosenfeld RM, Doerr T. 2015. Reporting of Postoperative Pain Management Protocols in Randomized Clinical Trials of Mandibular Fracture Repair: A Systematic Review. *JAMA Facial Plast Surg* 17:440-448.
- Champy M, Wilk A, Schneebelen JM. 1975. [Treatment of mandibular fractures by means of osteosynthesis without intermaxillary immobilization according to F.X. Michelet's technic]. Zahn-, Mund-, und Kieferheilkunde mit Zentralblatt 63:339-341.
- Choi BH, Kim KN, Kang HS. 1995a. Clinical and in vitro evaluation of mandibular angle fracture fixation with the two-miniplate system. *Oral Surgery, Oral Medicine, Oral Pathology, Oral Radiology and Endodontology* 79:692-695.
- Choi BH, Yoo JH, Kim KN, Kang HS. 1995b. Stability testing of a two miniplate fixation technique for mandibular angle fractures. An in vitro study. *Journal of Cranio-Maxillofacial Surgery* 23:122-125.
- Chrcanovic BR. 2013. Fixation of mandibular angle fractures: in vitro biomechanical assessments and computer-based studies. *Oral Maxillofac Surg* 17:251-268.
- Czerwinski M, Parker WL, Chehade A, Williams HB. 2008. Identification of mandibular fracture epidemiology in Canada: Enhancing injury prevention and patient evaluation. *The Canadian journal of plastic surgery = Journal canadien de chirurgie plastique* 16:36-40.
- Damm NB, Morlock MM, Bishop NE. 2015. Friction coefficient and effective interference at the implant-bone interface. *Journal of biomechanics* 48:3517-3521.

- Dechow PC, Panagiotopoulou O, Gharpure P. 2017. Biomechanical implications of cortical elastic properties of the macaque mandible. *Zoology (Jena, Germany)* 124:3-12.
- Dimitroulis G, Steidler N. 1992. Massive bleeding following maxillofacial trauma. Case report. *Aust Dent J* 37:185-188.
- Dongas P, Hall GM. 2002. Mandibular fracture patterns in Tasmania, Australia. *Australian Dental Journal* 47:131-137.
- Ellis E, Moos KF, El-Attar A. 1985. Ten years of mandibular fractures: An analysis of 2,137 cases. *Oral Surgery, Oral Medicine, Oral Pathology* 59:120-129.
- Ellis E, Walker L. 1994. Treatment of mandibular angle fractures using two noncompression miniplates. *Journal of oral and maxillofacial surgery* 52:1032-1036.
- Ellis E, Walker LR. 1996. Treatment of mandibular angle fractures using one noncompression miniplate. *Journal of Oral and Maxillofacial Surgery* 54:864-871.
- Fedok FG, Van Kooten DW, DeJoseph LM, McGinn JD, Sobota B, Levin RJ, Jacobs CR. 1998. Plating techniques and plate orientation in repair of mandibular angle fractures: an in vitro study. *Laryngoscope* 108:1218-1224.
- Fox AJ, Kellman RM. 2003. Mandibular angle fractures: two-miniplate fixation and complications. *Archives of facial plastic surgery* 5:464-469.
- Fuh LJ, Hsu JT, Huang HL, Chen MY, Shen YW. 2013. Biomechanical investigation of thread designs and interface conditions of zirconia and titanium dental implants with bone: three-dimensional numeric analysis. *The International journal of oral & maxillofacial implants* 28:e64-71.
- Gerlach KL, Schwarz A. 2002. Bite forces in patients after treatment of mandibular angle fractures with miniplate osteosynthesis according to Champy. *Int J Oral Maxillofac Surg* 31:345-348.
- Ghiasi MS, Chen J, Vaziri A, Rodriguez EK, Nazarian A. 2017. Bone fracture healing in mechanobiological modeling: A review of principles and methods. *Bone Rep* 6:87-100.
- Greenberg AM. 1993. Craniomaxillofacial Fractures : Principles of Internal Fixation Using the AO/ASIF Technique. New York, NY: New York, NY : Springer New York.
- Haug RH, Barber JE, Reifeis R. 1996. A comparison of mandibular angle fracture plating techniques. *Oral Surgery, Oral Medicine, Oral Pathology, Oral Radiology, and Endodontology* 82:257-263.
- Hente R, Lechner J, Fuechtmeier B, Schlegel U, Perren S. 2001. Der Einfluss einer zeitlich limitierten kontrollierten Bewegung auf die Frakturheilung. *Hefte Unfallchirurg* 283:23-24.
- Kopp RW, Crozier DL, Goyal P, Kellman RM, Suryadevara AC. 2016. Decade review of mandible fractures and arch bar impact on outcomes of nonsubcondylar fractures. *Laryngoscope* 126:596-601.
- Korioth TW, Hannam AG. 1994. Deformation of the human mandible during simulated tooth clenching. *J Dent Res* 73:56-66.
- Korioth TW, Romilly DP, Hannam AG. 1992. Three-dimensional finite element stress analysis of the dentate human mandible. *Am J Phys Anthropol* 88:69-96.
- Kraaij G, Zadpoor AA, Tuijthof GJ, Dankelman J, Nelissen RG, Valstar ER. 2014. Mechanical properties of human bone-implant interface tissue in aseptically loose hip implants. *Journal of the mechanical behavior of biomedical materials* 38:59-68.
- Kruger E, Heitz-Mayfield LJ, Perera I, Tennant M. 2010. Geographic modelling of jaw fracture rates in Australia: a methodological model for healthcare planning. *Dent Traumatol* 26:217-222.
- Liu YF, Fan YY, Jiang XF, Baur DA. 2017. A customized fixation plate with novel structure designed by topological optimization for mandibular angle fracture based on finite element analysis. *Biomed Eng Online* 16:131.
- MacLeod AR, Pankaj P, Simpson AH. 2012. Does screw-bone interface modelling matter in finite element analyses? *Journal of biomechanics* 45:1712-1716.

- Mehari Abraha H, Iriarte-Diaz J, Ross CF, Taylor AB, Panagiotopoulou O. 2019. The Mechanical Effect of the Periodontal Ligament on Bone Strain Regimes in a Validated Finite Element Model of a Macaque Mandible. *Frontiers in Bioengineering and Biotechnology* 7.
- Nasser M, Pandis N, Fleming PS, Fedorowicz Z, Ellis E, Ali K. 2013. Interventions for the management of mandibular fractures. *Cochrane Database Syst Rev*:CD006087.
- Nelson GJ. 1986. Three dimensional computer modeling of human mandibular biomechanics. In.
- Nikolaus A, Currey JD, Lindtner T, Fleck C, Zaslansky P. 2017. Importance of the variable periodontal ligament geometry for whole tooth mechanical function: A validated numerical study. *Journal of the Mechanical Behavior of Biomedical Materials* 67:61-73.
- Orsbon CP, Gidmark NJ, Ross CF. 2018. Dynamic musculoskeletal functional morphology: integrating diceCT and XROMM. *The Anatomical Record* 301:378-406.
- Owens BD, Kragh JF, Wenke JC, Macaitis J, Wade CE, Holcomb JB. 2008. Combat Wounds in Operation Iraqi Freedom and Operation Enduring Freedom. *Journal of Trauma: Injury, Infection & Critical Care* 64:295-299.
- Panagiotopoulou O, Iriarte-Diaz J, Mehari Abraha H, Taylor AB, Wilshin S, Dechow PC, Ross CF. 2020. Biomechanics of the mandible of Macaca mulatta during the power stroke of mastication: Loading, deformation, and strain regimes and the impact of food type. *J Hum Evol* 147:102865.
- Panagiotopoulou O, Iriarte-Diaz J, Wilshin S, Dechow PC, Taylor AB, Mehari Abraha H, Aljunid SF, Ross CF. 2017. In vivo bone strain and finite element modeling of a rhesus macaque mandible during mastication. *Zoology (Jena, Germany)* 124:13-29.
- Passeri LA, Ellis E, Sinn DP. 1993. Complications of nonrigid fixation of mandibular angle fractures. *Journal of Oral and Maxillofacial Surgery* 51:382-384.
- Pena I, Jr., Roberts LE, Guy WM, Zevallos JP. 2014. The cost and inpatient burden of treating mandible fractures: a nationwide inpatient sample database analysis. *Otolaryngol Head Neck Surg* 151:591-598.
- Perren SM. 2002. Evolution of the internal fixation of long bone fractures. The scientific basis of biological internal fixation: choosing a new balance between stability and biology. *J Bone Joint Surg Br* 84:1093-1110.
- Ross CF, Berthaume MA, Dechow PC, Iriarte-Diaz J, Porro LB, Richmond BG, Spencer M, Strait D. 2011. In vivo bone strain and finite-element modeling of the craniofacial haft in catarrhine primates. *Journal of anatomy* 218:112-141.
- Rudderman RH, Mullen RL, Phillips JH. 2008. The biophysics of mandibular fractures: an evolution toward understanding. *Plastic and reconstructive surgery* 121:596-607.
- Schierle HP, Schmelzeisen R, Rahn B, Pytlik C. 1997. One- or two-plate fixation of mandibular angle fractures? *Journal of Cranio-Maxillofacial Surgery* 25:162-168.
- Schon R, Roveda SI, Carter B. 2001. Mandibular fractures in Townsville, Australia: incidence, aetiology and treatment using the 2.0 AO/ASIF miniplate system. *The British journal of oral & maxillofacial surgery* 39:145-148.
- Shetty V, McBrearty D, Fourney M, Caputo AA. 1995. Fracture line stability as a function of the internal fixation system: an in vitro comparison using a mandibular angle fracture model. *Journal of Oral and Maxillofacial Surgery* 53:791-801; discussion 801-792.
- Shockley JS, von Fraunhofer JA, Seligson D. 1985. A measurement of the coefficient of static friction of human long bones. *Surface Technology* 25:167-173.
- Siddiqui A, Markose G, Moos KF, McMahon J, Ayoub AF. 2007. One miniplate versus two in the management of mandibular angle fractures: a prospective randomised study. *The British journal of oral & maxillofacial surgery* 45:223-225.
- Sinclair AG, Alexander RM. 1987. Estimates of forces exerted by the jaw muscles of some reptiles. *Journal of Zoology* 213:107-115.

- Tams J, Van Loon J-P, Rozema F, Otten E, Bos P. 1996. A three-dimensional study of loads across the fracture for different fracture sites of the mandible. British Journal of Oral and Maxillofacial Surgery 34:400-405.
- Tate GS, Ellis E, 3rd, Throckmorton G. 1994. Bite forces in patients treated for mandibular angle fractures: implications for fixation recommendations. J Oral Maxillofac Surg 52:734-736.
- van den Bergh B, Heymans MW, Duvekot F, Forouzanfar T. 2012. Treatment and complications of mandibular fractures: a 10-year analysis. J Craniomaxillofac Surg 40:e108-111.
- van Eijden TM. 2000. Biomechanics of the mandible. Crit Rev Oral Biol Med 11:123-136.
- Voutat C, Nohava J, Wandel J, Zysset P. 2019. The Dynamic Friction Coefficient of the Wet Bone-Implant Interface: Influence of Load, Speed, Material and Surface Finish. Biotribology 17:64-74.
- Zachar MR, Labella C, Kittle CP, Baer PB, Hale RG, Chan RK. 2013. Characterization of mandibular fractures incurred from battle injuries in Iraq and Afghanistan from 2001-2010. J Oral Maxillofac Surg 71:734-742.

Figure Legends

Figure 1. Terminology. (A) Single plate (Champy) fixation. (B) biplanar fixation. The angle of the mandible (in purple) is at the junction between the ramus (in red) and corpus (in green).The symphysis is indicated by the dotted line and bordered on either side by the parasymphysis (in yellow). Labial (close to lip), lingual (close to tongue) and buccal (close to cheek) surfaces are indicated in black.

Figure 2: Flow chart of finite element analysis (FEA). (A) Patient specific Computed Tomography Scans were processed to (B) create 3D models of the healthy controls and (C) the fracture fixation angle treatments. (D) All models were assigned the same tissue material properties and boundary conditions to simulate post-canine chewing and (E) solved using Abaqus static implicit solvers.

Figure 3: Moments (Nm) acting about coronal sections through the mandible models during simulation of ipsilateral and contralateral chewing. Grey shading indicates fracture location.

Figure 4: (A) Maximum (ϵ_1 -positive values indicative of tension) and minimum (ϵ_3 -negative values indicative of compression) principal strain in the bone implant interface and fracture zone of the angle fracture fixation treatments (Champy, biplanar) and in the healthy control during ipsi- and contralateral chews. Scale bar indicates strain magnitudes in microstrain. Warm colors: larger positive strain magnitudes. Cold colors: larger negative strain magnitudes. Green: low strain magnitudes. (B) Differences in maximum (ϵ_1) and minimum (ϵ_3) principal strain magnitudes between healthy control and fracture models repaired with Champy or biplanar technique during chews ipsilateral or contralateral to fracture. Plates and screws are not included in comparisons. Scale bar: difference in microstrain between fixed and healthy models. White: no difference in strain magnitudes. Warm colours: larger strains in fixed than control model. Cold colours: lower strains in fixed than control model.

Figure 5: Percentage change in interfragmentary distance (IFD) between nodes across the fracture plane during chewing ipsi- and contralateral to the fracture in macaques. Warm and cold colours show areas with high and low IFD.

Figure 6: Differences in maximum (ϵ_1) and minimum (ϵ_3) principal strain magnitudes between healthy control and fracture models repaired with Champy or biplanar technique during chews ipsilateral or

contralateral to the fracture. Plates and screws not included in these comparisons. Scale bar: difference in microstrain between healthy control and fracture models. White: no difference in strain magnitudes. Warm colours: larger strains in fixed than control. Cold colours: lower strains in fixed than control.

Supplementary Information

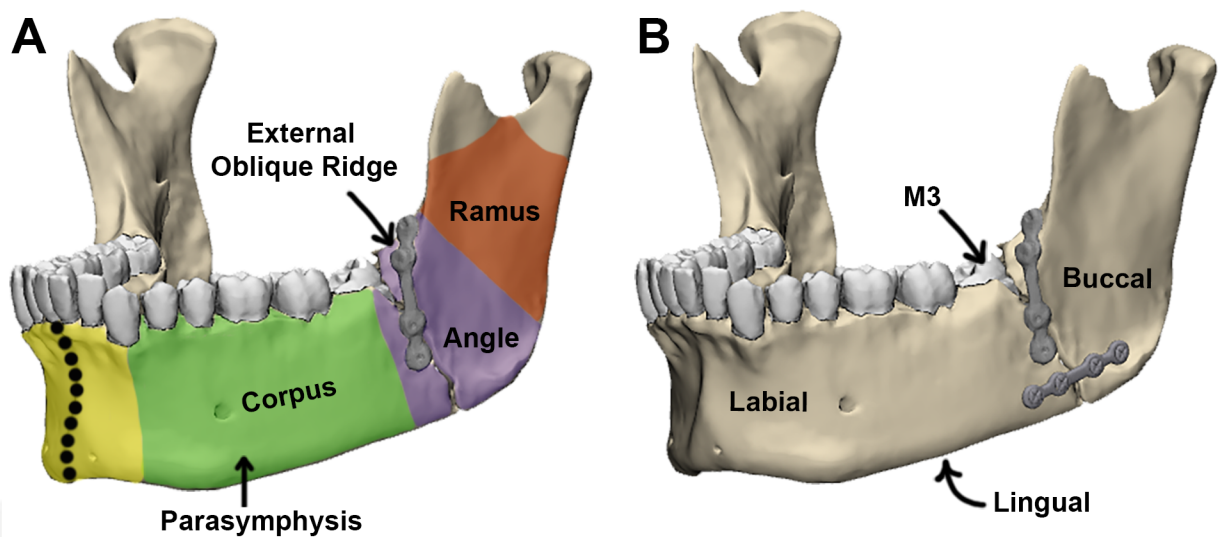
Supplementary Data 1: Muscle Force vectors used for all models

Supplementary Figure 1: 3D mesh of the bone interface and fracture zone of the Champy and Biplanar FE models.

Supplementary Figure 2. Von mises stress distribution at bone implant interface of all FEMs.

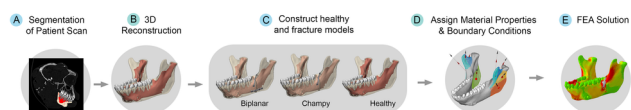
Supplementary Video 1: Animated GIFs of 20x deformation of macaque finite element models (FEMs) plotted with principal (ϵ_1 and ϵ_3) strains. FEMs are of the mandible in the healthy (unfractured) and angle fracture fixed (Champy and biplanar fixation) conditions under masticatory loads.

Accepted Article

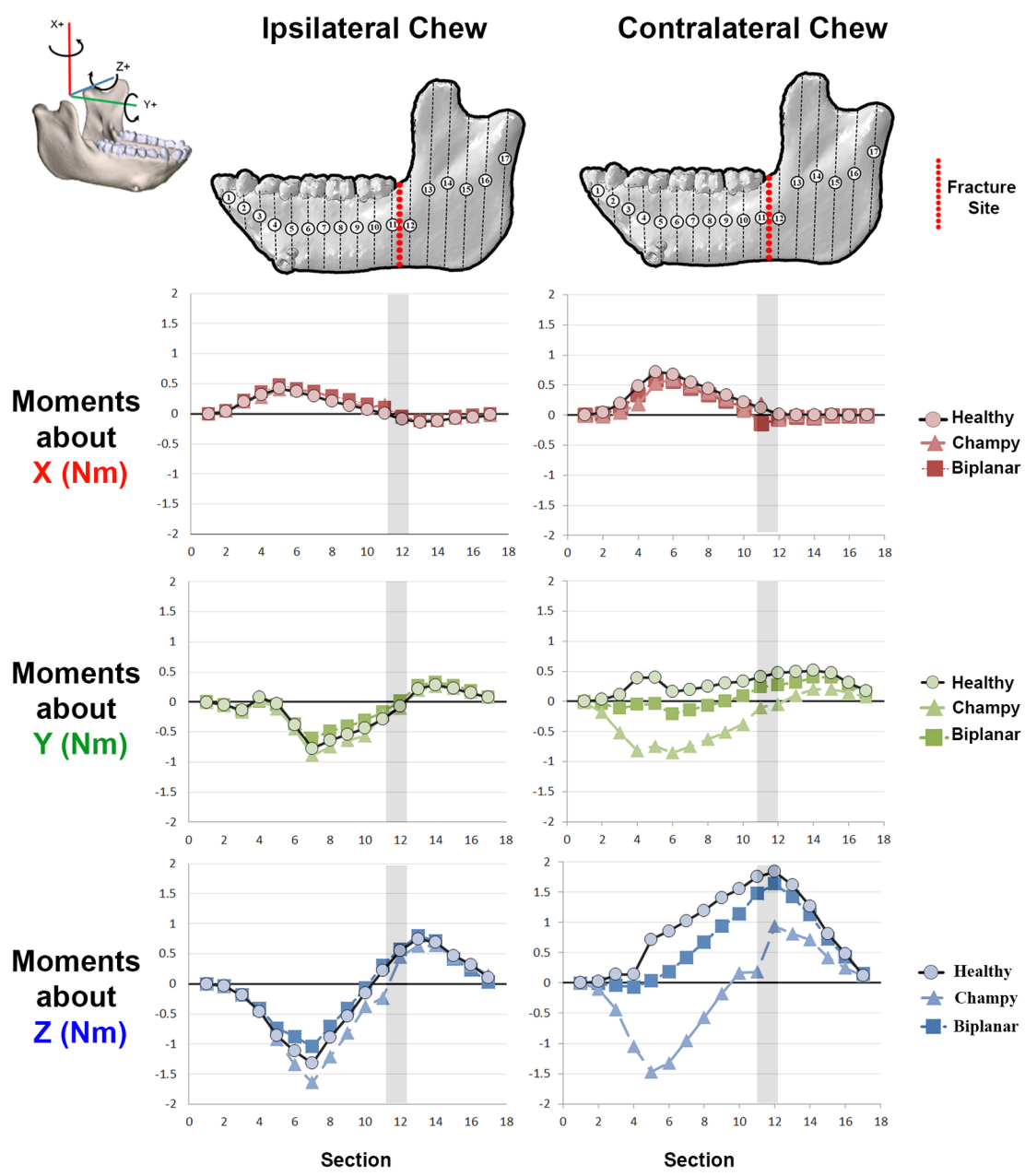


JBM4_10559_Figure 1.tif

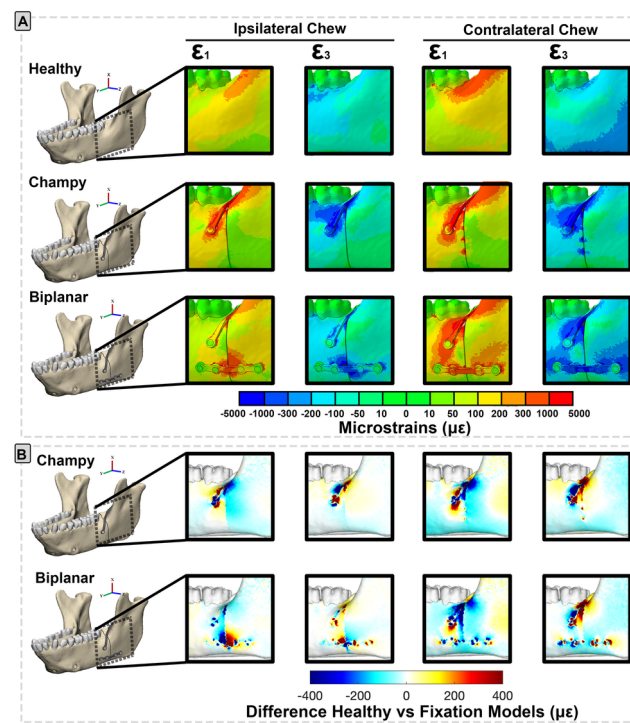
Accepted Article



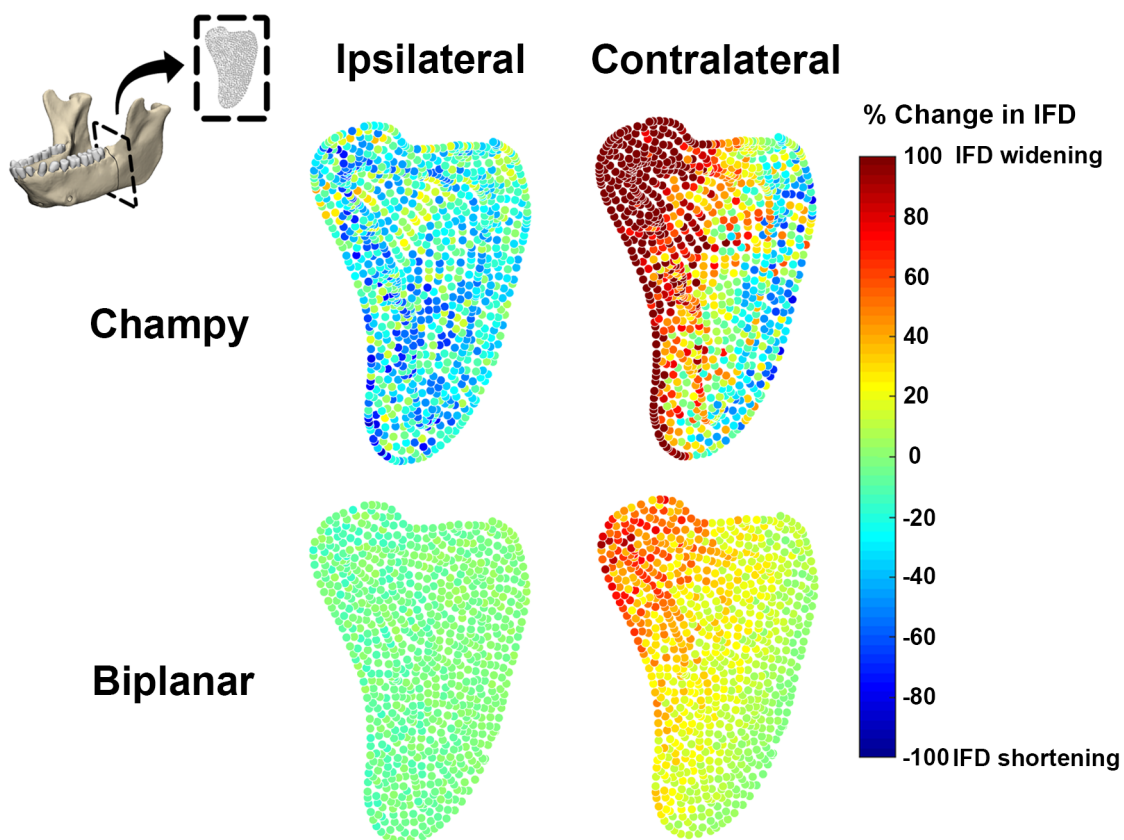
JBM4_10559_Figure 2.tif



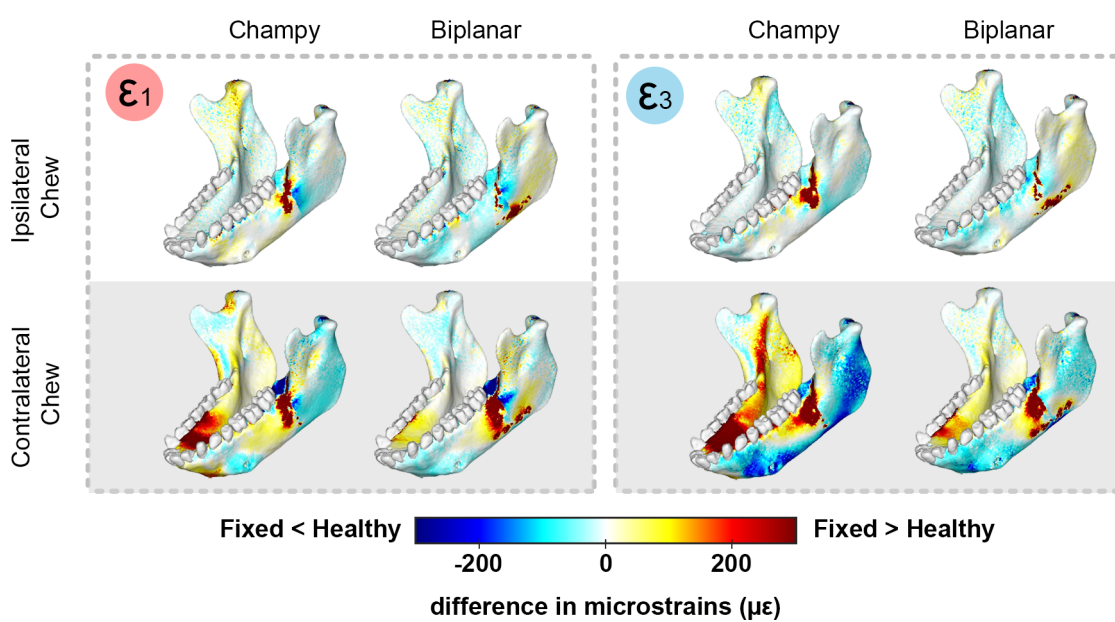
JBM4_10559_Figure 3.tif



JBM4_10559_Figure 4.tif



JBM4_10559_Figure 5.tif



JBM4_10559_Figure 6.tif